ORIGINAL REPORT



# Possible Clinical Effects of Ketoconazole on Sorafenib-induced Hand–Foot Skin Reaction and Cytoprotection Mechanisms of Antifungal Agents against Multikinase Inhibitor-induced Keratinocyte Toxicity

Rui KATO[1,2], Yayoi KAMATA[1], Mitsutoshi TOMINAGA[1], Ryoma KISHI[1,2], Takahide KANEKO[2], Akira TSUJIMURA[3], Yasushi SUGA[2] and Kenji TAKAMORI[1,2]

*[1]Juntendo Itch Research Center (JIRC), Institute for Environmental and Gender-Specific Medicine, Juntendo University Graduate School of Medicine, Chiba, [2]Department of Dermatology, Juntendo University Urayasu Hospital, Chiba, and [3]Department of Urology, Juntendo University Urayasu Hospital, Chiba, Japan*

**In recent years, molecular target drugs have become integral in treating malignant tumours. Multikinase inhibitors (MKIs) have been associated with serious skin disorders, including hand–foot skin reaction (HFSR), which impair patient quality of life, often disrupting activities of daily living necessitating dose reduction or discontinuation. As the pathogenic mechanisms of these skin disorders are unknown, no effective treatments have been established. Previously, by drug repurposing using an *in vitro* culture system, certain azole antifungal drugs (AFDs) were identified that prevented sorafenib-induced cell death of normal human epidermal keratinocytes. In this study, topical ketoconazole demonstrated clinical improvement in hyperkeratosis and pain associated with sorafenib-induced HFSR. Investigation of the mechanism using the *in vitro* culture system revealed sorafenib to be particularly cytotoxic among MKIs. Annexin V and TUNEL staining revealed apoptosis was mainly involved in this cytotoxicity. Antibody arrays and western blot showed increased levels of secretion of interleukin-1 receptor antagonist and macrophage migration inhibitory factor in culture supernatants. AFDs suppressed the secretion of these cytokines and reduced apoptosis in keratinocytes. This study reveals one aspect of the pathogenesis of sorafenib-induced HFSR and demonstrates that AFDs may be an effective treatment.**

*Key words:* multikinase inhibitor; antifungal drug; sorafenib; ketoconazole; itraconazole.

Submitted May 2, 2024. Accepted after revision Mar 13, 2025

Published Apr 28, 2025. DOI: 10.2340/actadv.v105.40697

Acta Derm Venereol 2025; 105: adv40697.

*Corr:* Kenji Takamori, MD, PhD, Juntendo Itch Research Center (JIRC), Institute for Environmental and Gender-Specific Medicine, Juntendo University Graduate School of Medicine, 2-1-1 Tomioka, Urayasu-shi, Chiba 279-0021, Japan. E-mail: ktakamor@juntendo.ac.jp

## SIGNIFICANCE

Hand–foot skin reaction, a common side effect of anticancer drugs including multikinase inhibitors, causes severe pain in the hands and feet, greatly impacting patients' quality of life. It often leads to dose reduction or treatment discontinuation due to its unclear cause. Effective treatments remain elusive, posing a significant challenge. This research delves into the mechanism of hand–foot syndrome induced by multikinase inhibitors and proposes certain antifungal drugs as potential therapies, resulting in advancing the development of treatments for hand–foot skin reaction significantly.

Molecular-targeted drugs, increasingly used to treat malignant tumours, selectively inhibit molecules critical for tumour growth and proliferation (1). Multikinase inhibitors (MKIs), targeting kinases including vascular endothelial growth factor receptor (VEGFR) and platelet-derived growth factor receptor (PDGFR), are typical molecular-targeted drugs. Certain MKIs, including sorafenib and sunitinib, have been associated with hand–foot skin reaction (HFSR) incidence rates of up to 33.8% and 18.9%, respectively (2). HFSR causes painful skin symptoms and abnormal sensations in the palms and soles, which cause difficulty in grasping and walking that impede quality of life (QOL), requiring dose reduction or cessation (3, 4). While treatments such as topical steroids and moisturizers are used, their efficacy is limited (2). However, HFSR correlates with favourable responses to sorafenib and sunitinib (5, 6), suggesting that addressing HFSR may enhance both QOL and treatment continuity in MKI-treated patients.

The pathogenesis of MKI-induced HFSR remains unclear. Histopathology of sorafenib-induced HFSR (7) shows keratinocyte degeneration, indicating MKI involvement in abnormal differentiation of normal human epidermal keratinocytes (NHEK). Preliminary data suggest that azole antifungal drugs (AFDs), including itraconazole, suppress sorafenib-induced keratinocyte toxicity *in vitro* (8), suggesting their potential to attenuate HFSR *in vivo*. This study investigates the effects of topical AFDs in 2 patients with sorafenib-induced HFSR and examines the role of MKIs in keratinocyte cytotoxicity and the protective effect of AFDs *in vitro*.

## MATERIALS AND METHODS

### *Participants*

As topical itraconazole is unavailable in Japan, ketoconazole cream was used as an alternative. Twice-daily application of topical ketoconazole cream (Nizoral 2%, Janssen Pharmaceuti-

cal, Beerse, Belgium) was administered to the soles of 2 patients with sorafenib-induced HFSR. Skin conditions were assessed monthly using visual analogue scale (VAS) scores for hyperkeratosis, erythema, blistering, and scaling, by 3 independent dermatologists blinded to patient identifiers and photograph dates. Blum's classification was applied for HFSR grading, and patients rated pain severity using the pain numeric rating scale (NRS). Topical steroids were discontinued 2 weeks before ketoconazole treatment. Prior to ketoconazole initiation, direct microscopy with 10% potassium hydroxide (KOH) excluded tinea pedis and fungal infection, but fungal cultures were not performed, which is a limitation. Written informed consent was obtained, and patients could withdraw at any time for any reason. The study was approved by Juntendo Urayasu Hospital Ethics Committee (No.2-085) and conducted in accordance with the Declaration of Helsinki.

*Reagents and antibodies*

Anti-IL-1α (rabbit polyclonal, P01583), anti-IL-1RA (rabbit monoclonal, EPR6483), anti-MIF (rabbit polyclonal, EPR12463), and anti-cIAP1 (rabbit monoclonal, EPR4673) antibodies were from Abcam (Cambridge, UK). Anti-cleaved caspase-3 (rabbit polyclonal, P42574), anti-PAI-1 (rabbit monoclonal, P05121), anti-caspase-1 (rabbit monoclonal, P29466), anti-caspase-8 (rabbit monoclonal, Q14790), anti-NFκB p65 (mouse monoclonal, Q04206), anti-phospho-NFκB p65 (rabbit monoclonal, Q04206), and the Death Receptor Antibody Sampler Kit II (containing anti-Fas, anti-TNFR1, anti-TRAILR1, anti-TRAILR2) were purchased from Cell Signaling Technology (Danvers, MA, USA). Z-DEVD-FMK (ZDEVD) and Z-VAD-FMK (ZVAD) were from Selleck Chemicals (Houston, TX, USA). Lenvatinib was from MedChem Express (Monmouth Junction, NJ, USA); sorafenib from Santa Cruz Biotechnology (Dallas, TX, USA); ketoconazole and itraconazole from Sigma-Aldrich (Saint Louis, MO, USA); sunitinib from Tocris Bioscience (Bristol, UK); regorafenib from Tokyo Chemical Industry (Tokyo, Japan); and capecitabine from Toronto Research Chemicals (Toronto, Canada). Halt protease inhibitor cocktail, horseradish peroxidase (HRP)-conjugated goat anti-rabbit IgG (H+L), Mammalian Protein Extraction Reagent, and Superclonal recombinant secondary antibody were from Thermo Fisher Scientific (Waltham, MA, USA).

*Cell culture*

NHEK derived from adult epidermis were purchased from Lonza (Basel, Switzerland) and cultured in keratinocyte basal medium (KBM)-Gold with keratinocyte growth medium-Gold SingleQuots (Lonza) at 37°C in 5% $CO_2$.

*Cell counting kit (CCK)-8 assay*

MKIs with/without caspase inhibitors (ZVAD, ZDEVD) or anticancer drugs (sorafenib, regorafenib, sunitinib, lenvatinib, capecitabine) were added to KBM-Gold at final concentrations of 1, 3, 5, 7 or 10 μM, and incubated overnight at 37°C with 5% $CO_2$. After washing twice with phosphate-buffered saline (PBS), cells were treated with CCK-8 reagent (Dojindo, Kumamoto, Japan) and incubated for 3 h at 37°C. Cell viability was measured at 450 nm using an ARVO X4 Multi-label Plate Reader (Perkin Elmer, Waltham, MA, USA).

*Antibody array*

Sub-confluent NHEK cells were treated with each MKI concentration and incubated overnight at 37°C. Culture supernatants and cell lysates were collected. Cells were lysed with Mammalian Protein Extraction Reagent (M-PER) containing Halt protease inhibitor cocktail and incubated at 4°C for 30 min. After centrifugation at 14,000 rpm for 5 min, the supernatants were used as cell lysates. Cytokine expression levels were analysed with Proteome Profiler Cytokine and Apoptosis Array Kits (R&D Systems, Minneapolis, MN, USA) per manufacturer instructions. Spot densities were measured using NIH Image J program.

*Western blot*

Equal amounts of total protein (3 μg) were loaded onto e-PAGEL15% (ATTO, Tokyo, Japan) and electrophoresed at 20 mA/gel for 70 min. Proteins were transferred to an Immobilon-P PVDF membrane (Millipore, Burlington, MA, USA) using Powered Blot (ATTO). Membranes were blocked with Block Ace (KAC, Kyoto, Japan) for 1 h at room temperature, then incubated overnight at 4°C with primary antibodies (Anti-IL-1α, anti-IL-1RA, anti-MIF, anti-PAI-1, anti-cIAP-1, anti-cleaved caspase-3, anti-caspase-1, anti-caspase-8, anti-TRAILR1, anti-TRAILR2, anti-Fas, anti-TNFR1, anti-NFκB p65, and anti-phospho NFκB p65). After 3 Tris Buffered Saline with Tween (TBST) washes, membranes were incubated for 1 h at room temperature with HRP-conjugated goat anti-rabbit IgG (H+L) and superclonal recombinant secondary antibody. Bands were detected using SuperSignal West Pico PLUS Chemiluminescent Substrate (Thermo Fisher Scientific) with an Amersham Imager 600 (GE Healthcare, Marlborough, MA, USA). Anti-β-actin (ProteinTech, Rosemont, IL, USA) served as the internal control. Relative band densities were analysed using NIH ImageJ.

*ELISA*

IL-1α in the supernatant of NHEK treated with sorafenib (7 μM) and AFD (1 μM) was measured using the Quantikine™ ELISA Human IL-1α/ IL-1F1 Immunoassay Kit (R&D Systems) as per manufacturer instructions. Spot densities were analysed with NIH ImageJ.

*Detection of apoptotic cells*

Annexin V-positive apoptotic cells were identified using the Apoptotic/Necrotic/Healthy Cells Detection Kit (PromoCell, Heidelberg, Germany). Subconfluent NHEK were treated with sorafenib (7 μM), ketoconazole (1 μM), and/or itraconazole (1 μM) overnight. After 2 washes with binding buffer (an isotonic buffer containing calcium), cells were stained with FITC-annexin V, EthD-III, and Hoechst 33342 incubated in the dark for 15 min, and imaged using a BZ-X800 fluorescence microscope (Keyence, Osaka, Japan).

Terminal deoxynucleotidyl transferase dUTP nick end labelling (TUNEL)-positive cells were detected using the *in situ* Cell Death Detection Kit (Takara, Shiga, Japan). Treated NHEK were washed, fixed with 4% paraformaldehyde, permeabilized, and incubated with the TUNEL reaction mixture. After washing with PBS, cells were mounted in Vectashield Mounting Medium with DAPI (Vector Laboratories, Newark, CA, USA) and analysed using the same microscope.

*Statistical analysis*

Statistical analyses were performed using Prism 9 (GraphPad Software, San Diego, CA, USA). For cell viability measurements, 6 independent biological replicate experiments were conducted, while all other experiments were performed in triplicate. The dots in each graph represent individual acquisitions. Data are shown as mean ± SD. One-way or two-way ANOVA, followed by Dunnett's or Tukey's test, was used where appropriate. Statistical significance was defined as $p < 0.05$.

## RESULTS

### *Clinical effects of topical ketoconazole on HFSR*

The clinical efficacy of topical ketoconazole for treating HFSR was evaluated in 2 patients:

*Patient 1:* An 84-year-old male with no history of dermatological diseases, receiving sorafenib for renal cell carcinoma with a good therapeutic response. Before ketoconazole application, he had been using urea cream (**Table I**). He presented with hyperkeratotic lesions on the toes, plantar surfaces, and heels (**Fig. 1A,** Fig. S1A). Topical ketoconazole, applied twice daily for 1 month, led to visible improvement (Fig. S1E). Continued treatment for an additional two months further reduced hyperkeratotic lesions (Fig. 1B**,** Fig. S1B), with corresponding improvements in NRS and hyperkeratosis skin scores (**Table II**).

*Patient 2:* An 81-year-old male, also with no history of dermatological diseases, receiving sorafenib for renal cell carcinoma with a good therapeutic response. Before ketoconazole application, he had been using topical steroids (Table I). He presented with hyperkeratosis on the toes, soles, and heels despite steroid use (Fig. 1C, Fig. S1C). Topical ketoconazole therapy was initiated, and progressive improvement was observed mainly in the lesions on the soles of the feet (Fig. 1D, Fig. S1D, S1F). This was particularly evident at 3 and 6 months. Skin scoring confirmed marked improvement, with reduced NRS scores and severity of hyperkeratosis (Table II).

### *Cytotoxicity of MKIs and capecitabine against NHEK*

The cytotoxicity of various MKIs (lenvatinib, regorafenib, sunitinib) and the anticancer drug capecitabine against NHEK was assessed. Neither MKIs nor capecitabine significantly reduced cell viability compared with the control (dimethyl sulfoxide: DMSO) across tested concentrations. However, sorafenib showed the strongest dose-dependent cytotoxicity (**Fig. 2**), accompanied by morphological changes in keratinocytes (Fig. S2A, B). Subsequent experiments used sorafenib at 7 μM, which reduced cell viability to 22%.

**Table I. Patient profiles and summary of sorafenib-induced HFSR**

| Data | Patient 1 | Patient 2 |
|---|---|---|
| Age, sex | 84 years, male | 81 years, male |
| Cancer type, sorafenib dose | RCC, 400 mg | RCC, 400 mg |
| Initial tumour response | Tumour burden | Tumour burden |
| Sorafenib before HFSR onset | 8 weeks | 8 weeks |
| Ketoconazole started | 6 months | 11 months |
| HFSR clinical features | Painful HK on soles and toes. ADL not disrupted. | Painful HK on soles and toes; erythema on soles; ADL disrupted |
| Pre-ketoconazole treatment | 10% urea cream | Topical steroid ointment |
| Follow-up period, why stopped | 3 months, symptoms relieved | 12 months, end of scheduled period |

RCC: renal cell carcinoma; HK: hyperkeratosis; HFSR: hand–foot skin reaction; ADL: activities of daily living.

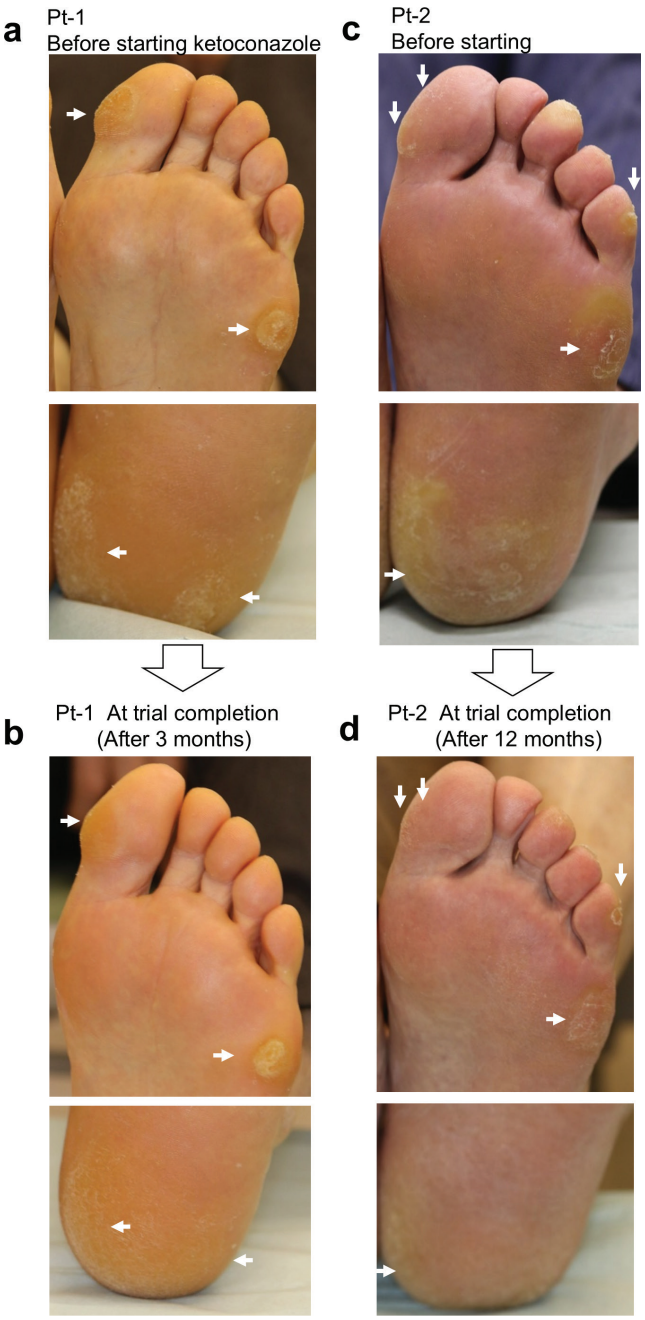


**Fig. 1. Clinical presentation of soles and heels in hand–foot skin reaction patients before and after ketoconazole cream treatment.** (A, B) Patient No. 1: 84-year-old male, clinical presentation of the soles and heels. (C, D) Patient No. 2: 81-year-old male, clinical presentation of the soles and heels. (A, C) Before ketoconazole treatment. (B, D) After ketoconazole treatment. Pt: Patient.

### *Evaluation of sorafenib-induced cytotoxicity*

Sorafenib increased Annexin V-positive cells, indicative of early apoptosis, compared with vehicle controls. However, co-treatment with AFDs significantly reduced Annexin V-positive cells (**Fig. 3**A). In the sorafenib group, mostly Annexin V-positive cells were co-stained with EthD-III, suggesting progressive apoptosis, while EthD-III positive cells not co-stained with Annexin V,

**Table II. HFSR grade severity of 4 skin symptoms and pain during treatment course**

| Data for patient numbers 1 and 2 | | Topical ketoconazole treatment course (months) | | | | | | | | | | | | | At trial completion |
|---|---|---|---|---|---|---|---|---|---|---|---|---|---|---|---|
| | | 0 | 1 | 2 | 3 | 4 | 5 | 6 | 7 | 8 | 9 | 10 | 11 | 12 | |
| 1 | Hyperkeratosis | 5.9 | 5.2 | 4.8 | 3.3 | | | | | | | | | | 3.3 |
| | Erythema | 2.5 | 2.6 | 2 | 1.8 | | | | | | | | | | 1.8 |
| | Bulla | 0 | 0 | 0 | 0 | – | – | – | – | – | – | – | – | – | 0 |
| | Desquamation | 1.5 | 1.1 | 0.8 | 0.5 | | | | | | | | | | 0.5 |
| | NRS | 20 | 10 | 5 | 5 | | | | | | | | | | 5 |
| | Severity | G1 | G1 | G1 | G1 | | | | | | | | | | G1 |
| 2 | Hyperkeratosis | 7 | 4.5 | 3 | 2.4 | 2.6 | 2.4 | 2.3 | 2.5 | 2.6 | 2.4 | 2.6 | 3.2 | 2.8 | 2.8 |
| | Erythema | 4.6 | 4.2 | 5.3 | 3.8 | 3.2 | 2.8 | 3.3 | 3.3 | 3.8 | 3.7 | 4.4 | 4.7 | 3.8 | 3.8 |
| | Bulla | 0 | 0 | 0 | 0 | 0 | 0 | 0 | 0 | 0 | 0 | 0 | 0 | 0 | 0 |
| | Desquamation | 1.4 | 0.3 | 1.2 | 0.7 | 0.5 | 0.6 | 0.6 | 0.7 | 0.5 | 0.6 | 0.4 | 0.9 | 0.7 | 0.7 |
| | NRS | 50 | 50 | 30 | 20 | 30 | 20 | 20 | 20 | 20 | 20 | 20 | 20 | 20 | 20 |
| | Severity | G2 | G2 | G2 | G1 | G2 | G1 | G1 | G1 | G1 | G1 | G1 | G1 | G1 | G1 |

Scoring of HFSR has not been established, other than Blum's classification. Four items, which often arise in multikinase inhibitor induced HFSR, were evaluated: hyperkeratosis, bulla, erythema, and desquamation. Evaluations according to VAS were made from photographs by dermatologists blinded to patient identity and therapy timing. NRS: numeric rating scale of pain severity rated by patients from 0 to 100, with 0 = no pain ~ 100 = pain as bad as it could be or worst imaginable; Blum's classification grades rated by 3 dermatologists (G1 = HFSR with only dysesthesia or unpleasant feeling in palms or soles, G2 = with pain disrupting activities of daily living; G3 = with intense pain restricting activities of daily living); VAS: visual analogue scale of symptom severity rated by 3 dermatologists from 0 min ~ 10 max.

indicating necrosis, were observed in the ketoconazole + sorafenib group (Fig. 3B, Fig. S3).

Sorafenib also increased TUNEL-positive cells, indicating DNA fragmentation in late apoptosis. Fewer TUNEL-positive cells were observed in the AFD+sorafenib group (approx. 0.4%) compared with the sorafenib group (approx. 5%) (Fig. 3C, Fig. S4).

### *Detection of apoptosis-related factors*

Apoptosis antibody arrays revealed changes in protein expression in sorafenib- and AFD-treated NHEK (Fig. S5). Sorafenib reduced TNFRI expression (Figs. S5, S6). *Tumour necrosis factor (TNF)-related apoptosis-inducing ligand-receptor (TRAILR)* -1, -2, and Fas also showed reduced expression in antibody arrays but not in western blotting (Figs S5, S6). Sorafenib decreased cIAP-1, an apoptosis suppressor, compared with vehicle (**Fig. 4A**), but itraconazole+sorafenib restored its expression (Fig. 4A). However, no significant difference in cIAP-1 expression was detected among other groups (Fig. 4B). Cleaved caspase-3 was observed in antibody arrays but not detected by western blotting under these conditions (Fig. 4C; Fig. S5B). Caspase-1 and caspase-8 expression and activation were unchanged by sorafenib (Figs. S6, S7). There was no change in cell viability with or without DMSO, confirming that the DMSO used for drug dissolution did not affect the measurement of cell viability for sorafenib and other drugs. Furthermore, neither the pan-caspase inhibitor ZVAD nor the caspase-3 inhibitor ZDEVD mitigated sorafenib-induced cytotoxicity in CCK-8 assays under these conditions (Fig. 4D). Based on the apoptosis array results and cell viability assays with caspase inhibitors, we hypothesize that sorafenib-induced keratinocyte apoptosis might be mediated by reduced cIAP1 expression, leading to NFκB activation in a caspase-independent manner. We further evaluated NFκB activation in sorafenib-induced cell death through Western blot analysis, which showed a dose-dependent increase in NFκB activity (Fig. S8).

### *Cytokine detection after sorafenib treatment*

Cytokine antibody arrays identified altered expression of interleukin (IL)-1α, IL-1 receptor antagonist (RA),

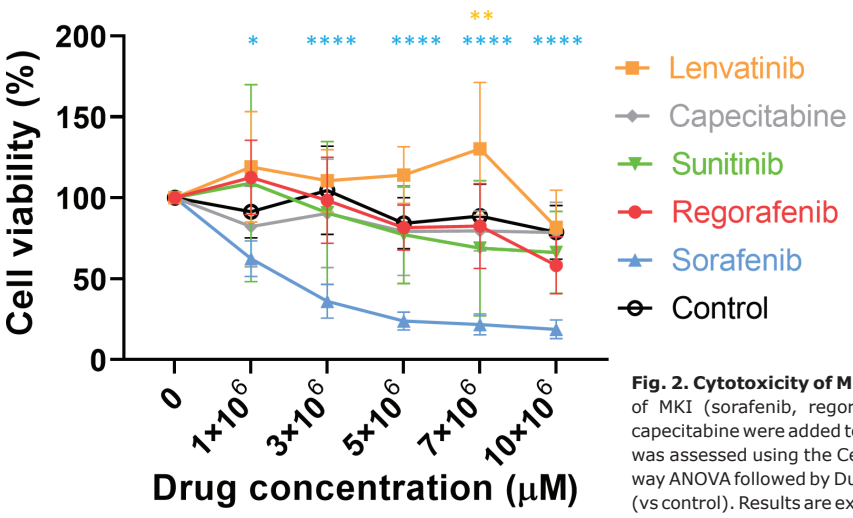


**Fig. 2. Cytotoxicity of MKI and capecitabine in NHEK.** Various concentrations of MKI (sorafenib, regorafenib, lenvatinib, sunitinib) or the anticancer drug capecitabine were added to cultured NHEK. After overnight incubation, cell viability was assessed using the Cell Counting Kit-8 assay. Data were analysed using two-way ANOVA followed by Dunnett's test; ****$p < 0.0001$, **$p < 0.01$ and *$p < 0.05$ (vs control). Results are expressed as the mean ± SD of quadruplicate experiments.

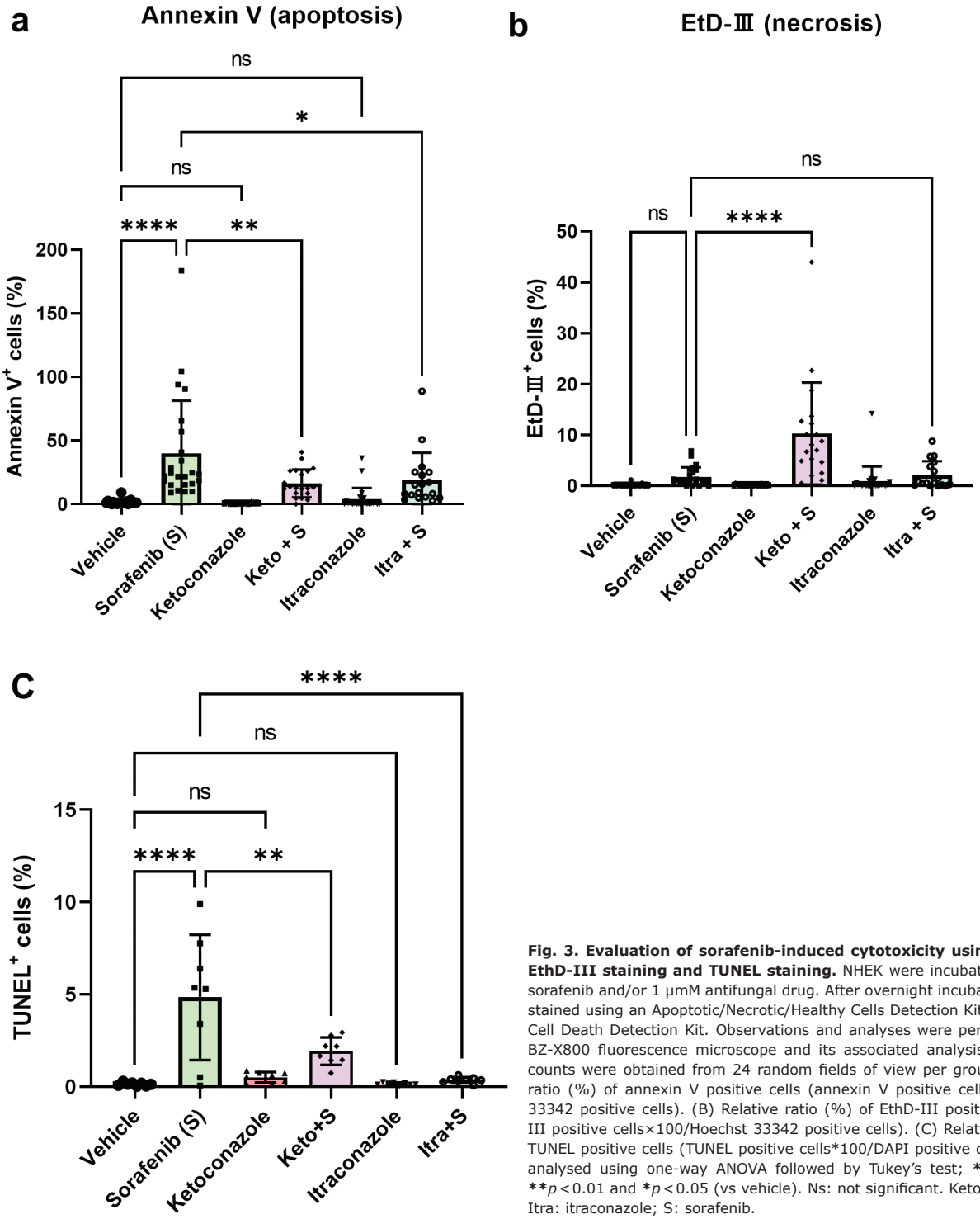


**Fig. 3. Evaluation of sorafenib-induced cytotoxicity using annexin V/EthD-III staining and TUNEL staining.** NHEK were incubated with 7 μmM sorafenib and/or 1 μmM antifungal drug. After overnight incubation, cells were stained using an Apoptotic/Necrotic/Healthy Cells Detection Kit and the *in situ* Cell Death Detection Kit. Observations and analyses were performed using a BZ-X800 fluorescence microscope and its associated analysis software. Cell counts were obtained from 24 random fields of view per group. (A) Relative ratio (%) of annexin V positive cells (annexin V positive cells×100/Hoechst 33342 positive cells). (B) Relative ratio (%) of EthD-III positive cells (EthD-III positive cells×100/Hoechst 33342 positive cells). (C) Relative ratio (%) of TUNEL positive cells (TUNEL positive cells*100/DAPI positive cells. Data were analysed using one-way ANOVA followed by Tukey's test; ****$p < 0.0001$, **$p < 0.01$ and *$p < 0.05$ (vs vehicle). Ns: not significant. Keto: ketoconazole; Itra: itraconazole; S: sorafenib.

macrophage migration inhibitory factor (MIF), and plasminogen activator inhibitor (PAI)-1 in cell lysates and supernatants of sorafenib-treated NHEK (Fig. S9A–I). IL-1α was detected in supernatants of sorafenib and ketoconazole+sorafenib groups. ELISA indicated significant differences compared with vehicle (**Fig. 5A, B**). IL-1RA and MIF increased in supernatants from sorafenib-treated NHEK and reduced by AFDs, especially itraconazole (Fig. 5C, D). Inflammatory cytokines such as TNFα, CXCL8, and IL-1β were not detected in either the cell lysate or the culture supernatant in this experiment.

PAI-1 decreased in supernatants of sorafenib and AFD+sorafenib groups compared with vehicle (Fig. S9E). Cytokine levels in cell lysates showed no significant difference among groups (Figs S9F–I, S10A–C, E).

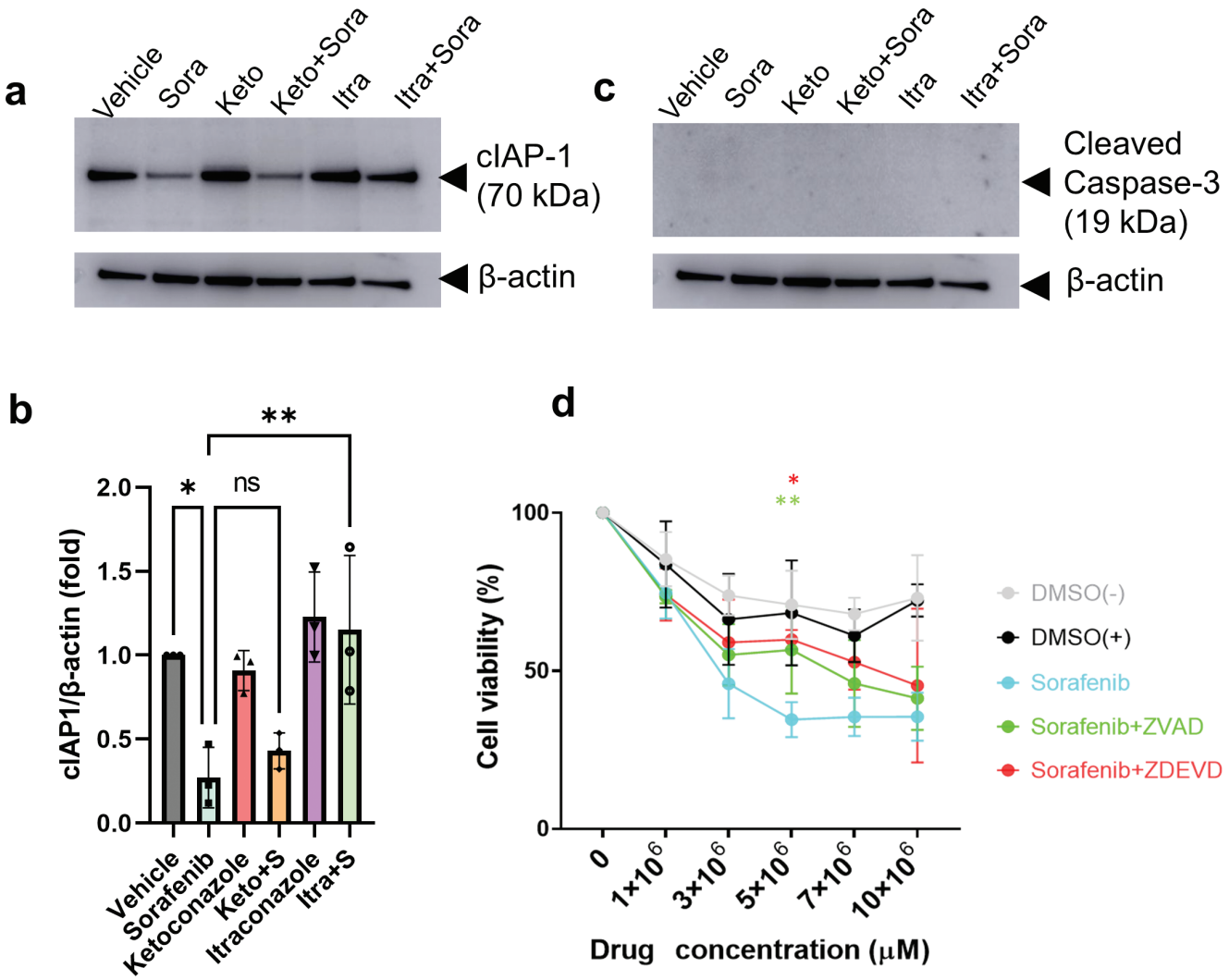


**Fig. 4. Detection of apoptosis-related factors in NHEK cell lysates following sorafenib and antifungal drug treatment.** Detection of (A) cIAP-1 (70 kDa) and (C) cleaved caspase-3 (19 kDa) in the cell lysate was performed using western blotting. (B) Bands were semi-quantified using ImageJ, and data were expressed as the relative ratio of cIAP-1/β-actin. Statistical analysis was conducted using one-way ANOVA followed by Tukey's test; ns indicates not significant. Sora or S: sorafenib, Keto: ketoconazole, Itra: itraconazole. All results are presented as the mean ± SD of triplicate experiments. (D) Various concentrations of sorafenib, with or without 50 μmM ZVAD or ZDEVD, were added to cultured NHEK cells. DMSO was used as the solvent for both sorafenib and the inhibitors. After overnight incubation, cell viability was assessed using the cell-counting kit-8 assay. Statistical analysis was performed using one-way ANOVA followed by Dunnett's test; $^{**}p < 0.01$ and $^{*}p < 0.05$ (vs DMSO (-)).

## DISCUSSION

In addition to their antifungal properties, AFDs exhibit antitumour effects, anti-inflammatory activity, and efficacy against various conditions including infantile haemangioma (10), castration-resistant prostate cancer, and Cushing's syndrome (11, 12). Ketoconazole has been reported to exacerbate mitophagy and induce apoptosis in hepatocellular carcinoma, with its cytotoxicity and effects potentially varying depending on the cell type (13). Hence, AFDs may prove effective against diseases beyond fungal conditions through diverse mechanisms of action.

Among MKIs, sorafenib is a prominent inducer of HFSR, targeting VEGFR, PDGFR, Raf, Kit, and other kinases associated with angiogenesis and tumour cell growth (14). In addition to these functions, sorafenib induces apoptosis in tumour cells by inhibiting extracellular signal-regulated kinase phosphorylation (15). This kinase inhibition may affect not only tumour cells but vascular endothelial and other cell types.

Our cell viability assay revealed that sorafenib exhibited high cytotoxicity among MKIs, suggesting a potential link between keratinocyte toxicity and HFSR development. During early apoptosis, annexin V binds to phosphatidylserine on the outer cell membrane (16), while EthD-III, a nucleic acid probe impermeable to intact membranes, stains cells based on membrane permeability. Positivity for EthD-III indicates necrotic cells or late-stage apoptotic cells with compromised membrane integrity (17). The higher rate of annexin V and EthD-III co-staining compared with EthD-III alone suggests that sorafenib-induced cytotoxicity is primarily

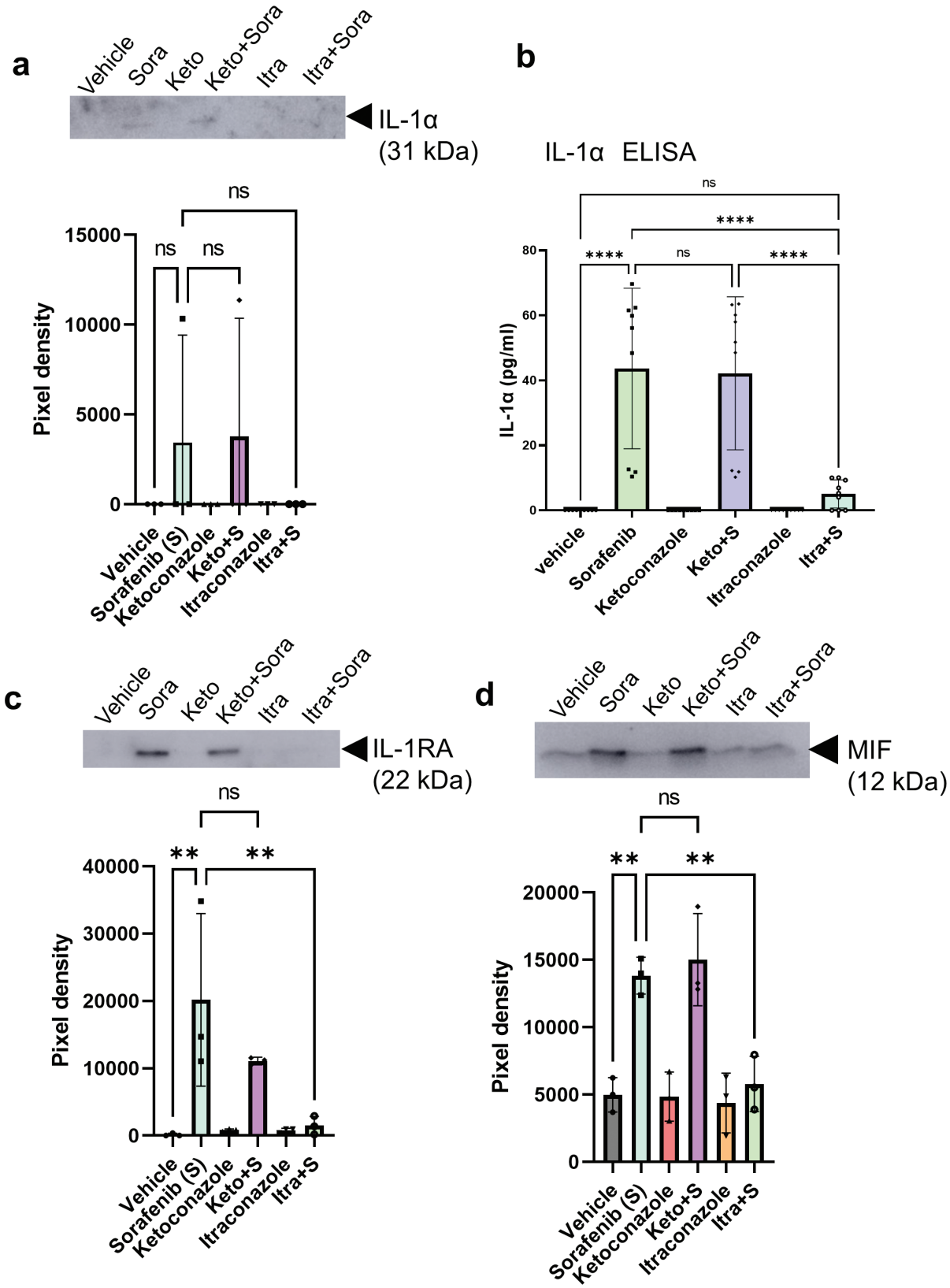


**Fig. 5. Detection of cytokines in culture supernatants of NHEK after sorafenib treatment.** (A) Western blot analysis and (B) ELISA of secretory IL-1α (31 kDa) in the culture supernatant. (C) Western blot analysis of secretory IL-1RA (20-25 kDa) in the culture supernatant. (D) Western blot analysis of secretory MIF (12 kDa) in the culture supernatant. Bands were semi-quantified using ImageJ and are presented as pixel density. Data were analysed using one-way ANOVA followed by Tukey's test. Statistical significance: ****$p < 0.0001$, **$p < 0.01$; ns: not significant. Abbreviations: Sora or S, sorafenib; Keto, ketoconazole; Itra, itraconazole. Results are presented as mean±SD from triplicate experiments.

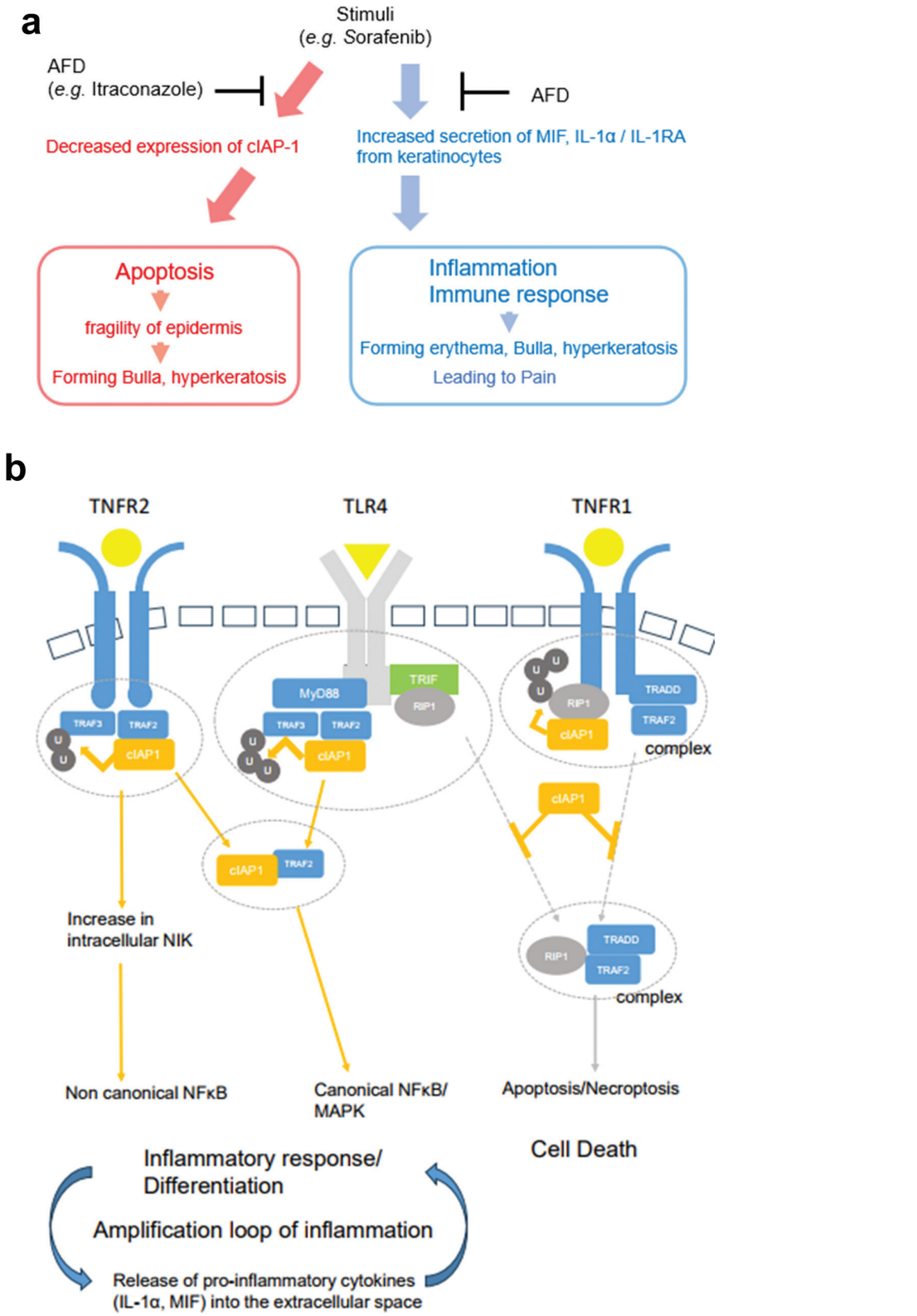


**Fig. 6. Mechanisms of cytotoxicity by sorafenib and the point of action of antifungal drug (AFD).** (A) Proposed clinical effects and mechanisms of AFDs on sorafenib-induced keratinocyte cytotoxicity. (B) Regulation of inflammatory systems and cell death by cIAP-1. cIAP-1 plays a role in the ubiquitination of TNFR-related complexes and TRAF3 in TLR4-related signalling, contributing to inflammatory responses, cell differentiation via activation of the classical NFκB pathway, and apoptosis regulation. It also promotes the intracellular release of NIK, activating the non-classical NFκB pathway. AFDs inhibit the activation of these inflammatory pathways and cell death induced by sorafenib-mediated downregulation of cIAP-1 expression. Figure adapted and modified from Ref. 14. Myd88: myeloid differentiation primary response 88; NIK: NF-κB-inducing kinase; RIP1: receptor interacting serine/threonine kinase 1; TLR 4: toll-like receptor 4; TNFR2: tumour necrosis factor Receptor 2; TRADD: TNFR-associated death domain; TRIF: toll–interleukin 1 receptor domain-containing adaptor inducing IFN-β.

mediated by apoptosis. In TUNEL staining, positivity in the sorafenib group was relatively lower than in Annexin staining, likely because TUNEL detects DNA fragmentation in late apoptosis. Importantly, sorafenib suppressed cIAP-1, an apoptosis suppressor, while AFDs restored its expression. These findings suggest that AFDs exert cytoprotective effects on keratinocytes by counteracting sorafenib-reduced cIAP-suppression.

cIAP-1 is expressed in various cell compartments, including the plasma membrane, cytoplasm, and nucleus, across multiple cell types, including epithelial cells. It regulates intracellular signalling pathways (18). The IAP family, including cIAP-1 and cIAP-2, plays a crucial role in cell survival by inhibiting apoptosis and controlling the cell cycle. While X-linked IAP (XIAP) directly inhibits caspase activation, cIAP-1 and cIAP-2 modulate signalling pathways via cell death receptors instead of directly inhibiting caspases (19). Suppression of cIAP expression typically triggers external apoptotic signals via TNFα, leading to apoptosis through NFκB activation (20). Recent studies have implicated cIAP in multiple pathways, particularly NFκB activation (21), influencing intracellular signalling cascades, cell cycle regulation, and cell migration. In this study, sorafenib dose-dependently increased NFκB p65 phosphorylation, suggesting that sorafenib-induced keratinocyte death is mediated through NFκB activation. This idea may also be supported by our data indicating that AFD-mediated suppression of apoptosis appears to operate independently of caspase activation and death receptors such as TRAILR, Fas, and TNFR1.

Sorafenib treatment increased extracellular secretion of IL-1RA and MIF in cultured NHEK, which was suppressed by AFDs. IL-1α, IL-1RA and MIF, known as alarmins, function as upstream regulators of the inflammatory system. They accumulate in vascular endothelial and epithelial cells under steady-state conditions and are upregulated by growth factors, cytokines, and stress stimuli. IL-1RA competitively inhibits IL-1R, counteracting IL-1α (22), while membrane-bound IL-1α induces chemokines and IL-6 via macrophages, creating a positive feedback loop (23). MIF, secreted in response to UV light and oxidative stress, promotes TNFα and IL-8 production and is implicated in inflammatory pain and hyperkeratosis in HFSR. AFDs may improve these symptoms by inhibiting MIF secretion (24). PAI-1, whose expression was suppressed by sorafenib in the culture supernatant, is involved in intercellular adhesion and cell migration (25). Loss of plasminogen activation regulation on the cell membrane due to PAI-1 inhibition can impair adhesion and induce apoptosis (26). These findings suggest that decreased PAI-1 expression after sorafenib treatment may reduce adhesion capacity rather directly induce keratinocyte apoptosis.

Itraconazole was more effective than ketoconazole in reducing sorafenib-induced NHEK apoptosis and suppressing IL-1RA and MIF secretion, likely due to structural differences between the drugs. These findings suggest that AFDs are promising therapeutic options for HFSR by addressing apoptosis, keratinocyte differentiation, cytokine-mediated interactions, and external damage. This study focused on keratinocytes and did not examine interactions with fibroblasts, immune system cells, or other cell types. However, the release of inflammatory cytokines such as IL-1α from keratinocytes suggests that interactions with other cell types may play a significant role.

Combining AFDs or using them with topical medications could enhance treatment outcomes. In fact, our clinical study found that topical AFDs improved hyperkeratosis and pain in HFSR patients. Sorafenib-induced apoptosis, reduced cIAP-1 expression, and elevated IL-1α and MIF levels likely contribute to blistering, keratinization, erythema, and pain due to epidermal fragility and heightened inflammatory and immune responses (Fig. 6). However, as this study involved only 2 cases, larger scale, controlled, randomized trials are needed to validate these findings.

## ACKNOWLEDGEMENTS

The authors would like to thank thank David Price at English Services for Scientists in Hiroshima for proofreading the manuscript.

*Funding sources:* This work was partly supported by a research grant from TORAY Industries, Inc. (Tokyo, Japan) and a research scholarship from Maruho Co., Ltd (Osaka, Japan).

*IRB approval status:* The study was approved by Juntendo Urayasu Hospital Ethics Committee (No.2-085).

*The authors have no conflicts of interest to declare.*

## REFERENCES

1. Lee YT, Tan YJ, Oon CE. Molecular targeted therapy: treating cancer with specificity. Eur J Pharmacol 2018; 834: 188–196. https://doi.org/10.1016/j.ejphar.2018.07.034
2. Ancker OV, Krüger M, Wehland M, Infanger M, Grimm D. Multikinase inhibitor treatment in thyroid cancer. Int J Mol Sci 2019; 21: 10. https://doi.org/10.3390/ijms21010010
3. Balagula Y, Wu S, Su X, Feldman DR, Lacouture ME. The risk of hand foot skin reaction to pazopanib, a novel multikinase inhibitor: a systematic review of literature and meta-analysis. Invest New Drugs 2012; 30: 1773–1781. https://doi.org/10.1007/s10637-011-9652-2
4. Anderson R, Jatoi A, Robert C, Wood LS, Keating KN, Lacouture ME. Search for evidence-based approaches for the prevention and palliation of hand–foot skin reaction (HFSR) caused by the multikinase inhibitors (MKIs). Oncologist 2009; 14: 291-302. https://doi.org/10.1634/theoncologist.2008-0237
5. Wang P, Tan G, Zhu M, Li W, Zhai B, Sun X. Hand–foot skin reaction is a beneficial indicator of sorafenib therapy for patients with hepatocellular carcinoma: a systemic review and meta-analysis. Expert Rev Gastroenterol Hepatol 2018; 12: 1–8. https://doi.org/10.1080/17474124.2017.1373018
6. Michaelson MD, Cohen DP, Li S, Motzer RJ, Escudier B, Barrios CH, et al. Hand–foot syndrome (HFS) as a potential biomarker of efficacy in patients (pts) with metastatic renal cell carcinoma (mRCC) treated with sunitinib (SU). J Clin Oncol 2011; 29: 320. https://doi.org/10.1200/

jco.2011.29.7_suppl.320
7. Lacouture ME, Reilly LM, Gerami P, Guotart J. HFSR in cancer patients treated with the MKIs sorafenib and sunitinib. Ann Oncol 2008; 19: 1955–1961. https://doi.org/10.1093/annonc/mdn389
8. Kamata Y, Kato R, Tominaga M, Toyama S, Komiya E, Utsumi J, et al. Identification of keratinocyte cytoprotectants against toxicity by the multikinase inhibitor sorafenib using drug repositioning. JID Innov 2024; 4:100271. https://doi.org/10.1016/j.xjidi.2024.100271
9. Blum JL, Jones SE, Buzdar AU, LoRusso PM, Kuter I, Vogel C, et al. Multicenter phase II study of capecitabine in paclitaxel-refractory metastatic breast cancer. J Clin Oncol 1999; 17: 485–493. https://doi.org/10.1200/JCO.1999.17.2.485
10. Tsai YC, Tsai TF. Itraconazole in the treatment of nonfungal cutaneous diseases: a review. Dermatol Ther (Heidelb) 2019; 9: 271–280. https://doi.org/10.1007/s13555-019-0299-9
11. Tresnanda RI, Pramod SV, Safriadi F. Ketoconazole for the treatment of docetaxel-naïve metastatic castration-resistant prostate cancer (mCRPC): a systematic review. Asian Pac J Cancer Prev 2021; 22: 3101–3107. https://doi.org/10.31557/APJCP.2021.22.10.3101
12. Simões Corrêa Galendi J, Correa Neto ANS, Demetres M, Boguszewski CL, Nogueira VDSN. Effectiveness of medical treatment of Cushing's disease: a systematic review and meta-analysis. Front Endocrinol (Lausanne) 2021; 12: 732240. https://doi.org/10.3389/fendo.2021.732240
13. Chen Y, Chen HN, Wang K, Zhang L, Huang Z, Liu J, et al. Ketoconazole exacerbates mitophagy to induce apoptosis by downregulating cyclooxygenase-2 in hepatocellular carcinoma. J Hepatol 2019; 70: 66–77. https://doi.org/10.1016/j.jhep.2018.09.022
14. Wilhelm SM, Carter C, Tang L, Wilkie D, McNabola A, Rong H, et al. BAY 43-9006 exhibits broad spectrum oral antitumor activity and targets the RAF/MEK/ERK pathway and receptor tyrosine kinases involved in tumor progression and angiogenesis. Cancer Res 2004; 64: 7099–7109. https://doi.org/10.1158/0008-5472.CAN-04-1443
15. Liu L, Cao Y, Chen C, Zhang X, McNabola A, Wilkie D, et al. Sorafenib blocks the RAF/MEK/ERK pathway, inhibits tumor angiogenesis, and induces tumor cell apoptosis in hepatocellular carcinoma model PLC/PRF/5. Cancer Res 2006; 66: 11851–11858. https://doi.org/10.1158/0008-5472.CAN-06-1377
16. Atale N, Gupta S, Yadav UC, Rani V. Cell-death assessment by fluorescent and nonfluorescent cytosolic and nuclear staining techniques. J Microsc 2014; 255: 7–19. https://doi.org/10.1111/jmi.12133
17. Rieger AM, Nelson KL, Konowalchuk JD, Barreda DR. Modified annexin V/propidium iodide apoptosis assay for accurate assessment of cell death. J Vis Exp 2011; 50: 2597. https://doi.org/10.3791/2597-v
18. Zadoroznyj A, Dubrez L. Cytoplasmic and nuclear functions of cIAP1. Biomolecules 2022; 12: 322. https://doi.org/10.3390/biom12020322
19. Gill C, Dowling C, O'Neill AJ, Watson RW. Effects of cIAP-1, cIAP-2 and XIAP triple knockdown on prostate cancer cell susceptibility to apoptosis, cell survival and proliferation. Mol Cancer 2009; 8: 39. https://doi.org/10.1186/1476-4598-8-39
20. Varfolomeev E, Goncharov T, Fedorova AV, Dynek JN, Zobel K, Deshayes K, et al. c-IAP1 and c-IAP2 are critical mediators of tumor necrosis factor alpha (TNFalpha)-induced NF-kappaB activation. J Biol Chem 2008; 283: 24295–2429. https://doi.org/10.1074/jbc.C800128200
21. Kocab AJ, Duckett CS. Inhibitor of apoptosis proteins as intracellular signaling intermediates. FEBS J 2016; 283: 221–231. https://doi.org/10.1111/febs.13554
22. Onozaki K. Interleukin1: from cell growth control to chronic inflammatory diseases. Yakugaku Zasshi 2013; 133: 645–660. https://doi.org/10.1248/yakushi.13-00064
23. Di Paolo NC, Shayakhmetov DM. Interleukin 1α and the inflammatory process. Nat Immunol 2016; 17: 906–913. https://doi.org/10.1038/ni.3503
24. Alexander JK, Cox GM, Tian JB, Zha AM, Wei P, Kigerl KA, et al. Macrophage migration inhibitory factor (MIF) is essential for inflammatory and neuropathic pain and enhances pain in response to stress. Exp Neurol 2012; 236: 351–362. https://doi.org/10.1016/j.expneurol.2012.04.018
25. Providence KM, Higgins SP, Mullen A, Battista A, Samarakoon R, Higgins CE, et al. SERPINE1 (PAI-1) is deposited into keratinocyte migration "trails" and required for optimal monolayer wound repair. Arch Dermatol Res 2008; 300: 303–310. https://doi.org/10.1007/s00403-008-0845-2
26. Rossignol P, Ho-Tin-Noé B, Vranckx R, Bouton MC, Meilhac O, Lijnen HR, et al. Protease nexin-1 inhibits plasminogen activation-induced apoptosis of adherent cells. J Biol Chem 2004; 279: 10346–1356. https://doi.org/10.1074/jbc.M310964200